Journal of Power Sources 306 (2016) 70–77

Contents lists available at ScienceDirect

Journal of Power Sources

journal homepage: www.elsevier.com/locate/jpowsour

An investigation of functionalized electrolyte using succinonitrile additive for high voltage lithium-ion batteries

Renjie Chen [a, b, *], Fan Liu [a], Yan Chen [a], Yusheng Ye [a], Yongxin Huang [a], Feng Wu [a, b, **], Li Li [a, b]

[a] School of Materials Science & Engineering, Beijing Key Laboratory of Environmental Science and Engineering, Beijing Institute of Technology, Beijing 100081, China
[b] Collaborative Innovation Center of Electric Vehicles in Beijing, Beijing 100081, China

HIGHLIGHTS

- The SN-based electrolytes show better thermal stability and wider electrochemical window.
- The effects of SN on the electrochemical performances of LIBs have been investigated.
- The 1 wt % SN-containing electrolyte improves cycle performance of LNMO batteries.

GRAPHICAL ABSTRACT

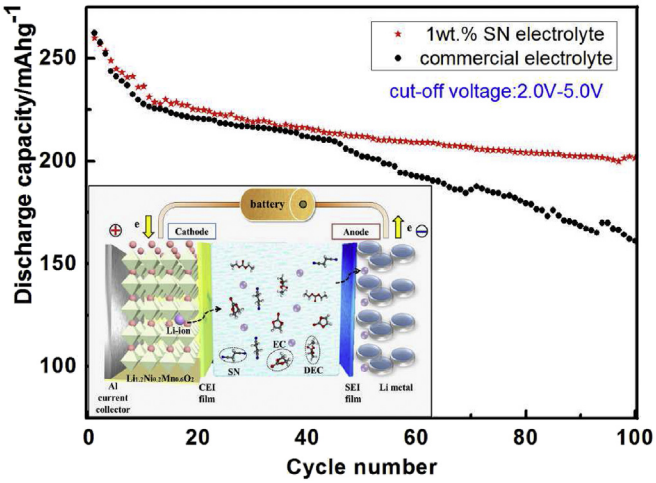

ARTICLE INFO

Article history:
Received 16 July 2015
Received in revised form
27 October 2015
Accepted 28 October 2015
Available online 13 December 2015

ABSTRACT

Succinonitrile (SN) has been used as functional additive to improve the thermal stability and broaden the oxidation electrochemical window of commercial electrolyte 1 M $LiPF_6$/EC/DEC (1:1, by volume) for high-voltage LIBs (cathode: $Li_{1.2}Ni_{0.2}Mn_{0.6}O_2$, anode: Li). 1 wt % SN-based electrolyte showed a wide electrochemical oxidation window of 5.4 V vs Li^+/Li and excellent thermal stability demonstrated by thermogravimetry (TG) and X-ray photoelectron spectroscopy (XPS), as well as theoretical analysis according to molecular orbital theory. The LNMO ($Li_{1.2}Ni_{0.2}Mn_{0.6}O_2$) battery with 1 wt % SN-based electrolyte showed better cyclability and capacity retention when charged to higher cut-off voltage. The improved battery performance is mainly attributed to the formation of uniform cathode electrolyte interface (CEI)

* Corresponding author. School of Materials Science & Engineering, Beijing Key Laboratory of Environmental Science and Engineering, Beijing Institute of Technology, Beijing 100081, China.
** Corresponding author. School of Materials Science & Engineering, Beijing Key Laboratory of Environmental Science and Engineering, Beijing Institute of Technology, Beijing 100081, China.
E-mail addresses: chenrj@bit.edu.cn (R. Chen), wufeng863@vip.sina.com (F. Wu).

http://dx.doi.org/10.1016/j.jpowsour.2015.10.105

Keywords:
Succinonitrile
High voltage
Thermal stability
Cathode electrolyte interface

formed by interfacial reactions between the LNMO cathode and electrolyte. The outcome of this work and the continuous research on this subject can generate critical knowledge for designing thermal stability electrolytes for large format lithium-ion batteries.

1. Introduction

Lithium-ion batteries (LIBs) have been widely used in portable electronic devices since their commercialization. To satisfy the forceful motive power requirement of electric vehicle (EVs), hybrid electric vehicles (HEVs) and smart grid, developing high-voltage LIBs is a key approach to promote the energy density [1]. Currently, high-voltage cathode materials such as $LiCoPO_4$ and $LiNiPO_4$ can approach to 5 V or even higher [2,3]. However, the increased upper voltage limit may adversely affect cycle performance of entire battery system owing to the conventional EC-based electrolyte decomposing over time when the charge voltage reaches up to 4.5 V (vs. Li/Li^+) [4]. Although oxidization potentials vs. Li/Li^+ of organic carbonate solvents are usually reported about 5 V, the transition-metal ions of electrode could accelerate the electrolytes decomposition as catalyst, causing irreversible capacity fading [5].

There are mainly two ways to improve high-voltage electrolyte, finding new stable solvents and searching for novel functional additives. Fluorinated solvents, nitrile compounds, sulfone compounds, and ionic liquids are normally studied as new solvent or co-solvent. Our research group has reported several studies about high-voltage electrolyte based on tetramethylene sulfone [6–8]. As for additives, LiBOB is usually used for high-voltage cathode additives [9]. And other organic additives include sulfonate esters, phosphides, electrochemically polymerized monomers, carboxyl anhydrides and some special ethers [1]. Xiaolin Liao demonstrated that the 1% trimethylsilyl (TMSB)-containing electrolyte is helpful to suppress the self-discharge of the charged $LiNi_{0.5}Mn_{1.5}O_4$ cathode results from the preferential oxidation of TMSB and the subsequent formation of a protective solid electrolyte interphase film [10]. H. Bouayad investigated glutaric anhydride (GA) as an electrolyte additive to improve the performances of $LiNi_{0.4}Mn_{1.6}O_4/Li_4Ti_5O_{12}$ cells, benefited from a passivation film at the surface of both electrodes formed by GA degradation [11].

Among various high-voltage cathode materials, $Li_{1.2}Ni_{0.2}Mn_{0.6}O_2$ is one of the most promising candidates which can provide much higher capacity than the traditional cathode materials such as $LiCoO_2$ and $LiMn_2O_4$ spinel [12–14]. However, the commercialized application of $Li_{1.2}Ni_{0.2}Mn_{0.6}O_2$ is hindered by challenges of voltage instability and capacity fading [15]. Furthermore, Ni and Mn also exhibit concentration partitions within the thin layer of surface reconstruction layer (SRL) in the cycled samples where Ni is almost depleted at the very surface of the SRL, indicating the preferential dissolution of Ni ions in the electrolyte [16].

$LiPF_6$ can be easily hydrolyzed when electrolyte exist water and acidic impurities [17]. As shown in Fig. 1, Nitriles can react with water in the acidic condition (H^+) as shown in the first two steps of the equation, then water content drops down which relieves the process of $LiPF_6$ decomposed into HF at the same time. In total, not only does it can eliminate H_2O and HF which would promote Mn/Ni dissolution from the cathode, but also reduce the side reaction due to the formation of non-electrochemical active amide ($RCONH_2$).

Above all, previous researches have proved that nitrile-based electrolytes are very suitable for high-voltage cathodes. Yaser proposed that glutaronitrile is suitable for high energy/power Li-ion batteries as a co-solvent in thermally and electrochemically stable electrolyte mixtures at 14th International Meeting on Lithium Batteries [18]. Ue demonstrated that adiponitrile (ADN) exhibit could resist electrochemical oxidation at voltage of 5 V vs saturated calomel electrode (~8.3 vs Li^+/Li) [19]. Masatoshi Nagaham found that the EC/DMC/sebaconitrile (25:25:50 v/v) electrolyte containing 1 M $LiBF_4$ exhibited high electrochemical stability at 6.0 V on a $LiFePO_4$ electrode [20]. There have been some investigations about succinonitrile (SN) already, mainly focused on the polymer electrolyte [21–23], but only a few papers about SN for liquid electrolyte additive have been published [24–26]. Y. S. Kim proved that SN additives could improve the thermal stability of $LiCoO_2$ cells and used as overdischarge protection additives. Gu-Yeon Kim and co-workers investigated the effects of succinonitrile on the impedance of $LiCoO_2$/Graphite pouch cells.

In this paper we studied succinonitrile (SN) as a commercial electrolyte additive to improve the cycling performance and thermal stability of the $Li_{1.2}Ni_{0.2}Mn_{0.6}O_2/Li$ system in high cut-off voltage. Furthermore, the charge–discharge capacities of $Li_{1.2}Ni_{0.2}Mn_{0.6}O_2/Li$ with different cut-off voltages has been studied, and the effect of SN on the performance of the cells and reactions for the LNMO cathode were also discussed.

2. Experimental

2.1. Preparation of electrolyte systems

The electrolyte of 1 M $LiPF_6$ dissolved in ethylene carbonate (EC): Diethyl carbonate (DEC) (1:1, by volume), which was purchased from Zhangjiagang Guotai Huarong Chemical New Material Co. Ltd (named commercial electrolyte). SN-based electrolytes were prepared simply by mixing succinonitrile (SN, 99%, J&K Chemical) with the prepared electrolyte in various weight ratios in an argon-filled glovebox (H_2O < 0.1 ppm, O_2 < 0.1 ppm, Mikrouna) and stirring for 24 h at room temperature, We have tested the water content of commercial electrolyte and 1wt % SN-based electrolyte by Karl-fisher method, 8.7 ppm and 7.6 ppm was measured respectively.

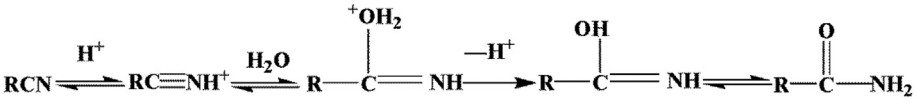

Fig. 1. The reaction mechanism of eliminating H_2O and HF by nitriles.

2.2. Preparation of the electrodes and the construction of cells

$Li_{1.2}Ni_{0.2}Mn_{0.6}O_2$ electrode material was prepared by coprecipitation according to the previous work [27]. The electrode consisted of $Li_{1.2}Ni_{0.2}Mn_{0.6}O_2$, acetylene black and PVDF in a weight ratio of 8:1:1, coating onto aluminum foil. The active mass loading was more than 1.8 mg/cm^2. The Li/$Li_{1.2}Ni_{0.2}Mn_{0.6}O_2$ coin-type half-cells (2025) were assembled in the argon-filled glovebox, and celgard 2400 was used as battery separator.

2.3. Electrochemical measurements

The electrolytes oxidation/reduction potentials were tested by an electrochemical workstation (CHI660E, Shanghai Chenhua Company) using a linear sweep voltammogram at a scan rate of 1 mV s^{-1} at 25 °C in the voltage range from −0.2 V to 6.0 V. The electrolyte was sealed in a glass cell. The working electrode is a platinum wire (99.9%, Ø = 0.1 mm) and the reference and counter electrode is Li foil (99.9%).

Electrochemical impedance spectra (EIS) were measured with a Zahner Elektrik IM6e impedance analyzer over the frequency range of 10^{-3} Hz ~ 10^6 Hz. The electrolyte ionic conductivity was tested by Pt conductance electrode from −30 °C to 80 °C in the programmable high-low temperature test chamber (GDJS-100, Wuxi Suoyate Company).

The thermal stability of the electrolytes was measured by using a thermal gravimetric analysis (TGA), performed with a Netzsch 209 F1 thermal analyzer. The samples (about 2 mL) used for measurements were filled and sealed in special aluminum pans, and temperature ranges from room temperature up to 600 °C at a scan rate of 10 °C min^{-1} under a nitrogen atmosphere.

The cell charge–discharge performance of the electrolytes were performing by Land battery testing system (CT2001A, Wuhan Lanhe Company) at room temperature, and the coin-type half-cells were galvanostatically cycled at a current density of 25 mAg^{-1} (corresponding to 0.1 C).

2.4. Materials characterizations

Morphological studies on the cathodes were investigated using a field emission scanning electron microscope (HITACHI S-3500N, Japan) with an accelerating voltage of 20 kV.

The surface species on the cycled cathodes was tested by X-ray photoelectron spectroscopy (XPS) using a chemical analysis (ESCA) spectrometer (PHI-1600, USA), radiated with a monochromatized Al-K_α (1486.6 eV) source, and the spectra results were analyzed by XPS-PEAK software.

3. Results and discussions

Fig. 2(a) shows the ion conductivity of the commercial electrolytes with different ratios of succinonitrile. The ionic conductivity of different ratios of SN electrolytes increased with the elevating temperature (−40 °C–80 °C), which is in agreement with Arrhenius law. The ionic conductivity of commercial electrolyte decreased as the succinonitrile amount increased. The ionic conductivity of the commercial electrolyte and 1wt % SN-based electrolyte at room temperature are 5.48 × 10^{-3} S cm^{-1} and 5.35 × 10^{-3} S cm^{-1} respectively.

Fig. 2(b) compares the electrochemical stability windows of the commercial electrolyte and 1wt % SN-based electrolyte by linear sweep voltammetry measurements. Comparing with the commercial electrolyte, the oxidation potential of electrolyte containing 1wt % SN rises from 5.0 V to 5.4 V, which can be explained well in the following calculation results. Although the oxidation potential of commercial electrolyte seems high (5 V), in fact, the actual voltage limits of the electrolyte are usually much lower than those obtained with an inert electrode because of the highly catalytic characteristic of the cathode materials [5]. And the trivial change guarantee the feasibility of the EC-DEC/SN mixed solvent for high voltage cathode materials.

The highest occupied molecular orbital (HOMO) energy level and the lowest unoccupied molecular orbital (LUMO) energy level can be calculated based on the molecular orbital theory, which reflects the ability to gain or lose electrons. Fig. 2(c) shows the frontier molecular orbitals of EC and DEC, as well as SN, and their energies are also shown using a B3LYP basis set. The energies of the LUMO and HOMO of SN (−0.30127 ha, −0.04180 ha) are both lower than those of EC (−0.25168 ha, −0.01248 ha) and DEC (0.23381 ha, 0.00220 ha). It indicates that SN molecules can accept electrons and possess a high oxidation potential, and the introduction of SN can also broaden the oxidation potential of the commercial electrolyte.

Fig. 2(d) shows the charge–discharge performance of Li/$Li_{1.2}Ni_{0.2}Mn_{0.6}O_2$ half-cells containing electrolyte with different ratios of succinonitrile. It is found that the electrolyte containing 1wt % SN achieved the best cycle performance. At the voltage range of 2.0–5.0 V, the cell with 1wt % SN-based electrolyte has a reversible discharge capacity of 223.8 $mAhg^{-1}$. Less SN cannot guarantee the oxidation potential improvement of the mix electrolyte, while redundant SN additives not only worsen the ionic conductivity but also may form a thick CEI layer, which also can be reflected by the following results of EIS.

The AC impedance spectra of Li/$Li_{1.2}Ni_{0.2}Mn_{0.6}O_2$ cells containing different ratios of SN electrolytes after the 1st and 5th cycles were measured as well (Fig. 3), and the inset graph shows the equivalent circuit of the examined cell. In Fig. 3, the AC impedance spectra shows a line with a slope in low frequency range, that is, the Warburg impedance (R_w), which is associated with Li-ion diffusion effects on the interface between the bulk phase of active material particles and electrolyte [28]. At high-middle frequency, the resistance value rises and falls to produce a semicircle section (R_{ct}), which is relevant for charge transfer phenomenon corresponding to film formation on the surface of the electrode [29]. In addition, C_{dl} represents the double layer capacitance at the interface between the working electrode and electrolyte, while the R_s is on behalf of the resistance of electrolyte, electrode, and separator. From Fig. 3(a), we can explore some patterns from the R_s value. The R_s value of the mixed electrolyte increased with the weight ratio of the SN, which may indicate the negative effects on the ionic conductivity after the addition of SN. Comparing the R_{ct} value of different electrolytes after 5 cycles (Fig. 3(b)), the 1wt % SN-based electrolyte has the minimum resistance. In fact, the R_{ct} value can reflect the electrodes corrosion rate [30], the commercial electrolyte has a higher R_{ct} value maybe caused by the deposition of Ni^{4+} and Mn^{4+} on the cathode, leading to the destruction of the cathode due to the manganese dissolution into electrolyte and the Jahn-Teller crystallographic distortion [31]. In the meantime, the electrolyte with redundant SN may form a thick CEI layer leading to a higher R_{ct} value. When taken all these experiment results into account, 1wt % SN-based electrolyte was believed to be the most optimal electrolyte system for the LNMO batteries.

Thermal stability and cycling performance at high temperature Fig. 4(a) and (b) and show the thermal stability of commercial electrolyte and 1wt % SN-based electrolyte. The TG profile indicates that both of two samples begin to lose weight from ambient temperature, but commercial electrolyte decays quickly. When the two samples decomposed 10% of onset amount, the temperature for 1wt % SN-based electrolyte (55.5 °C) is higher than commercial electrolyte (49.2 °C), this is mainly because of the thermal decomposition temperature of SN (267 °C) is higher than the two

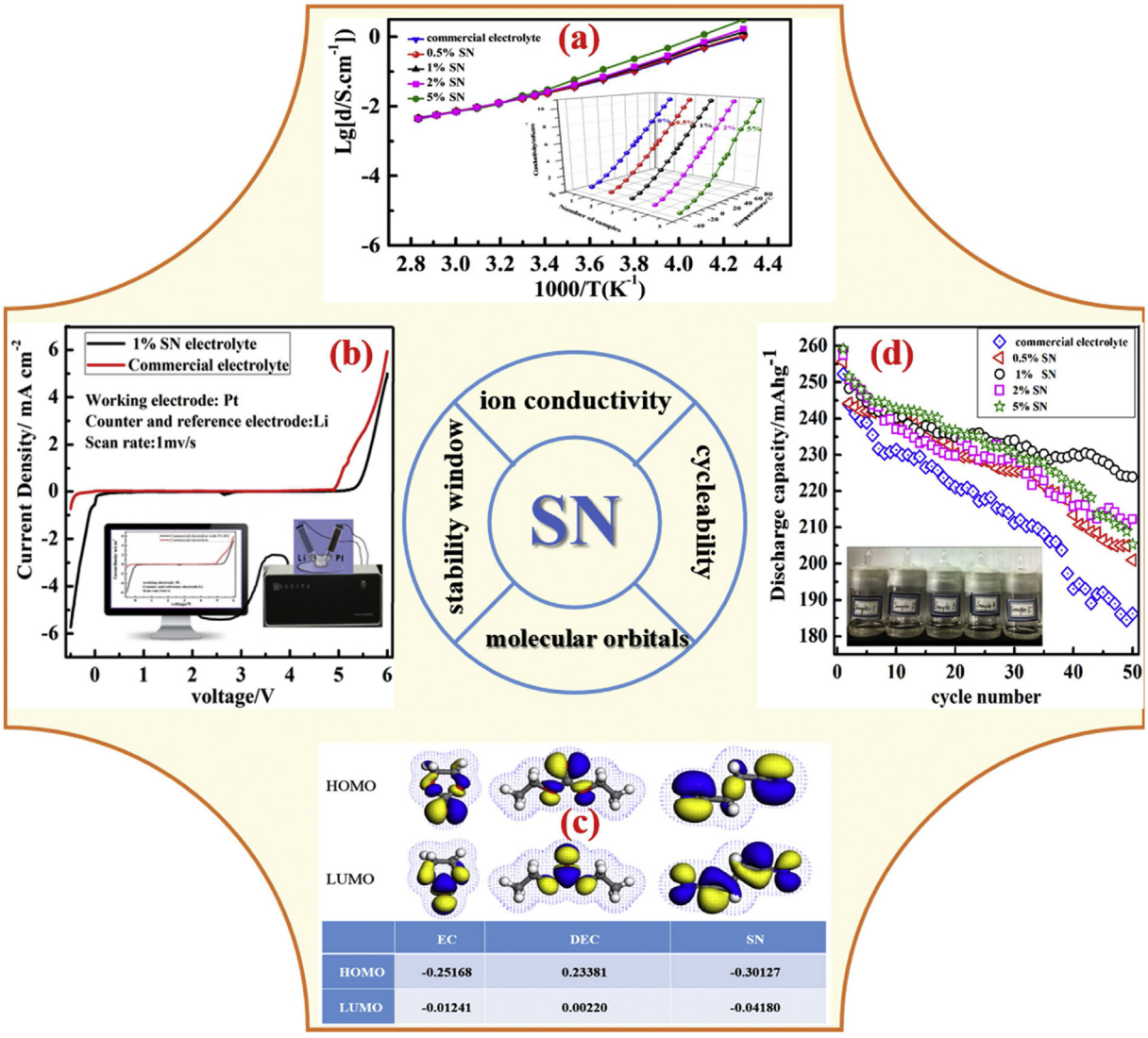

	EC	DEC	SN
HOMO	-0.25168	0.23381	-0.30127
LUMO	-0.01241	0.00220	-0.04180

Fig. 2. (a) The conductivity of commercial electrolytes containing different weight ratios of succinonitrile at temperatures range from −30 °C to 80 °C. (b) LSV of the 1 M LiPF6/EC/DEC commercial electrolyte with or without 1wt% SN. Working electrode: Pt, counter and reference electrodes: Li, scan rate: 1 mV s^{-1}. (c) Frontier molecular orbitals of EC, DEC and SN and their energies of occupied (HOMO) and unoccupied (LUMO) (in Ha). (d) Discharge capacity after 50 cycles of $Li/Li_{1.2}Ni_{0.2}Mn_{0.6}O_2$ half-cells containing various weight ratios of SN.

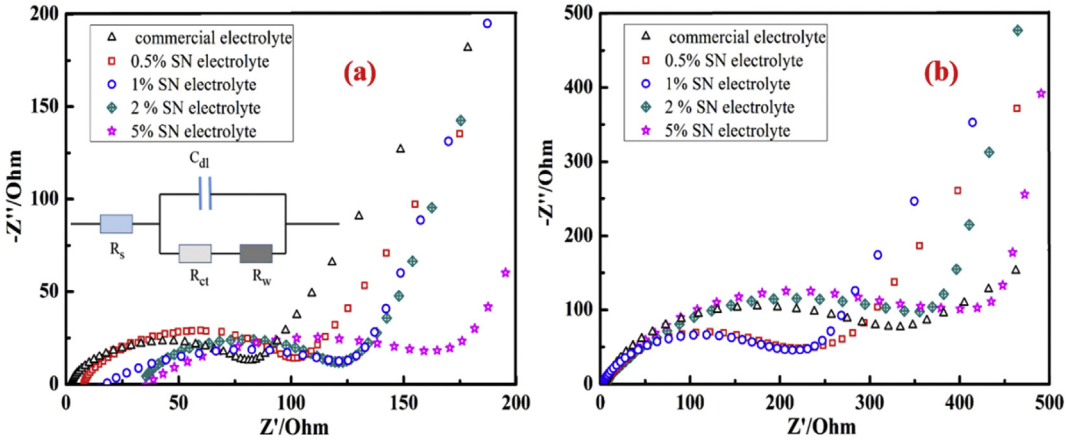

Fig. 3. Ac impedance spectra of the $Li/Li_{1.2}Ni_{0.2}Mn_{0.6}O_2$ half-cells containing various weight ratios of SN: (a) After 1 cycles, (b) After 5 cycles.

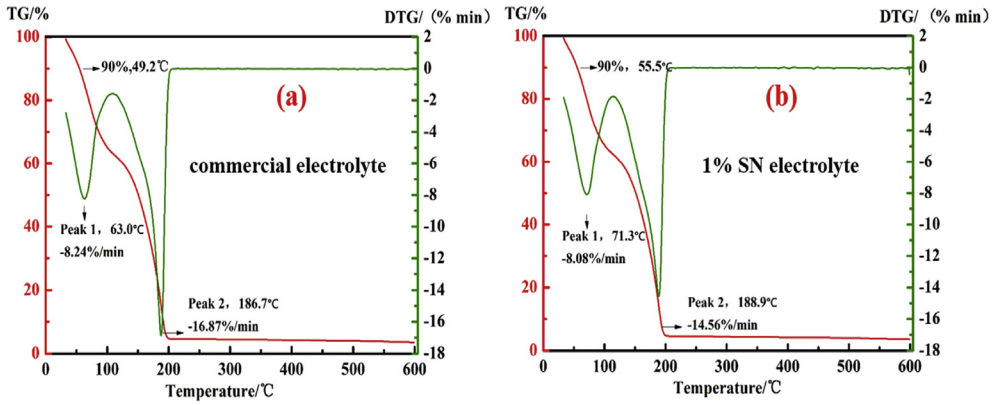

Fig. 4. TGA diagrams and DTG curves of commercial electrolyte (a) and 1wt % SN electrolyte (b).

main solvent EC (248 °C) and DEC (125.8 °C), the addition of SN leads to the tiny overall thermal stability improvement. The DTG profile shows the decomposition rate of the electrolyte, and the two peaks respectively represent the temperature for two mainly components (EC and DEC). From Fig. 3(a) and (b), it is obvious that decomposing temperature in two peaks for 1wt % SN-based electrolyte is higher, and the value of decomposing rate is smaller in the meantime. The results show that succinonitrile additive can improve the thermal stability of the commercial electrolyte.

To further clarify the thermal stability of the mixed electrolyte, the cycle performance of the half-cells at high temperatures (55 °C) has been investigated. The cells were placed in a battery-testing incubator and tested by a Land battery testing system at a voltage range of 2.0–4.8 V, at a current density of 0.1 C. As shown in Fig. 5, the initial discharge capacity of the Li/$Li_{1.2}Ni_{0.2}Mn_{0.6}O_2$ half-cell containing the 1wt % SN-based electrolyte is 268.7 $mAhg^{-1}$. After 50 cycles, the discharge capacity is higher than 240 $mAhg^{-1}$ and the coulombic efficiency is over 95% from the 2nd cycle. The discharge capacity of Li/$Li_{1.2}Ni_{0.2}Mn_{0.6}O_2$ half-cell with commercial electrolyte is less than 170$mAhg^{-1}$ after 50 cycles and retains only 66.8% of its initial capacity. The coulombic efficiency of the last few cycles is lower than 90%. By contrast, in the first few cycles, the coulombic efficiency of the cell containing the 1wt % SN-based electrolyte is lower than the cell with commercial electrolyte. It implies that SN-derived cathode electrolyte interface (CEI) forming in the first few cycles causes an irreversible capacity loss. The improvement in the thermal stability maybe due to the strong complex formation between the surface metal atoms of $Li_{1.2}Ni_{0.2}Mn_{0.6}O_2$ and nitrile (−CN) groups of SN except for the thermal stability improvement of electrolyte itself [25]. The inset shows the SEM images of the cathode surface with or without SN after 50 cycles. The inset on the right (1wt % SN) shows much more homogeneous CEI layer than the left inset (commercial electrolyte). The better CEI layer ensures the higher capacity retention of battery with electrolyte containing 1wt % SN.

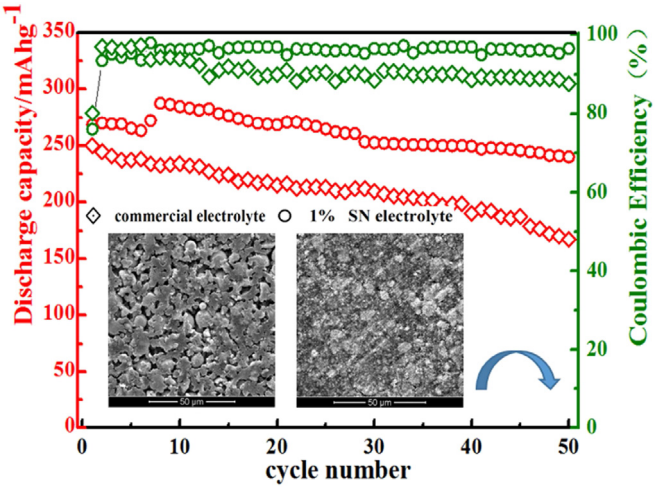

Fig. 5. Discharge capacities and coulombic efficiencies of the Li/Li1.2Ni0.2Mn0.6O2 half-cells at a 0.1 C current density with or without 1wt % SN at 55 °C, the inset displays SEM images of the batteries after 50 cycles.

Fig. 6 shows the discharge capacity of Li/$Li_{1.2}Ni_{0.2}Mn_{0.6}O_2$ half-cells with or without SN under different upper cut-off voltage. Fig. 6(a), (b), (c) and (d) are corresponding to 2.0–4.8 V, 2.0–4.9 V, 2.0–5.0 V and 2.0–5.2 V respectively. At all present cut-off voltage, the cycle performance of cell with 1wt % SN-based electrolyte is better than that with commercial electrolyte. When the cut-off voltage is between 2.0 and 4.8 or 4.9 V, they exhibited nearly identical cycling characteristics. When charging to 5.0 V, the discharge capacity of cell with 1wt % SN-based electrolyte can remain 223.8 $mAhg^{-1}$ after 50 cycles, while cell with commercial electrolyte discharge capacity drops to 186.2 $mAhg^{-1}$. It is due to the faster degradation rate of EC and DEC at higher voltage. The discharge capacity of cell with 1wt % SN-based electrolyte (2.0–5.2 V) decays faster than when they were charged to 5.0 V, but it is still much better than the cell with commercial electrolyte. The cell with commercial electrolyte nearly broke down after 20 cycles. These results demonstrate that the addition of succinonitrile to the electrolyte solution leads to a remarkably improved cycling stability, which is due to the formation of electronically conductive film on the cathode.

Fig. 7(a) and (b) display the SEM images of whole surface of $Li_{1.2}Ni_{0.2}Mn_{0.6}O_2$ with or without 1wt % SN after 5 cycles at a voltage range of 2.0–5.0 V. The cathode with succinonitrile forms a uniform surface layer which is called cathode electrolyte interface (CEI) [4]. The surface film formation is due to the reactions between the electrode material and the electrolyte, which also take place on the anode side of the LIBs, acting as protection layer. Usually the layer is detrimental for the cell because it leads to the performance degradation [17]. However, the performance of the LIBs depends on the mobility of the lithium ions in both electrodes and the electrolytes, thus the CEI really make a big significance especially in high-voltage cathode. It is clear that there is much difference in morphology between the cathode after 5 cycles with or without SN. Fig. 7(a) presents many fragments of LNMO particles, while Fig. 7(b) shows a much flatter cathode surface. It is clear to observe a thin and transparent CEI layer from the inset of Fig. 7(b).

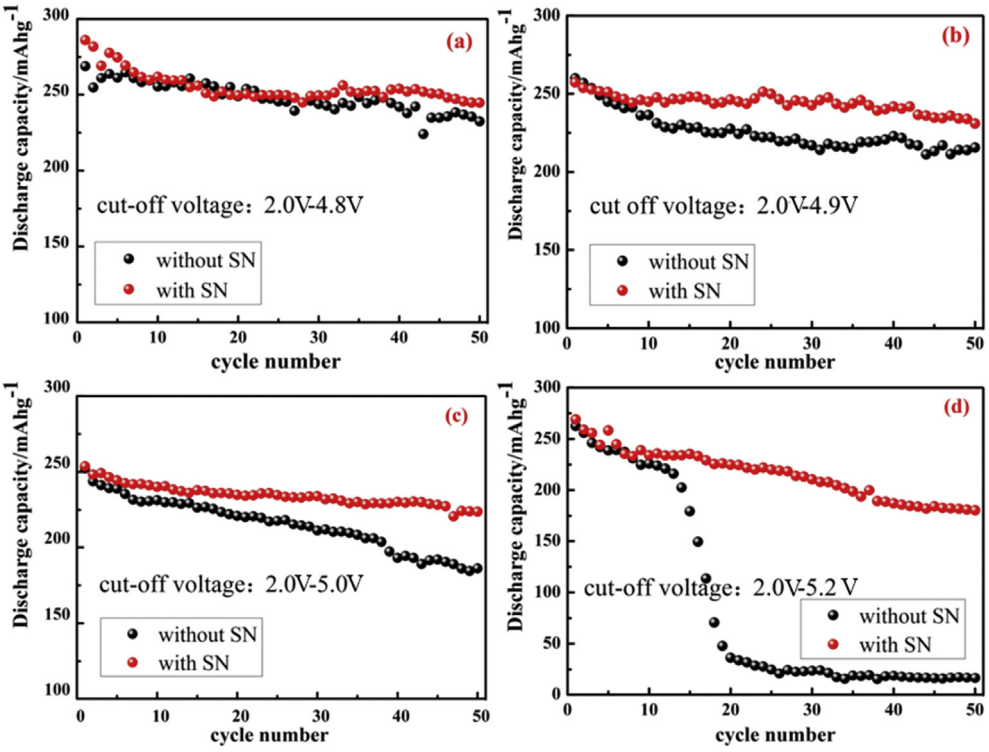

Fig. 6. Discharge capacities of $Li/Li_{1.2}Ni_{0.2}Mn_{0.6}O_2$ with 1wt% SN-based electrolyte at different cut-off voltages: (a) 2.0–4.8 V, (b) 2.0–4.9 V, (c) 2.0–5.0 V and (d) 2.0–5.2 V.

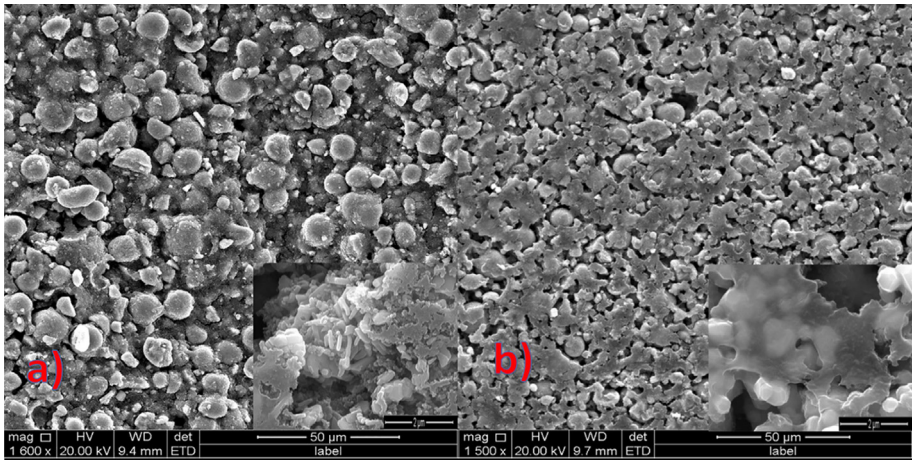

Fig. 7. SEM images of the surface of LNMO cathode after 5 cycles with: (a) commercial electrolyte (b) 1wt% SN.

Fig. 8 shows X-ray photoelectron spectroscopy (XPS) analysis data of the LNMO electrode after 50 cycles with and without SN. The N1s signal was clearly detected at 398.4 eV in the SN-containing sample, while the peak did not appear in its counterpart from the SN-absent cell shown in Fig. 8(b). The results indicate that SN is a part of species surface of the cathodes. Fig. 8(c) and (d) depict the Mn 2p spectra and the binding energy for both 2p3/2 and 2p1/2 orbital could be observed [32]. For the SN-absent sample, its 2p1/2 and 2p3/2 signals respectively located at 654 eV and 642 eV, suggesting a single valence of Mn^{4+}, which is consistent with earlier report. For the SN-containing sample, an obvious shift in 2p1/2 and 2p3/2 signal was observed. The shoulder peaks appear in the signal for both states, and the binding energy of the shoulder peaks indicate the presence of Mn^{3+}. The Ni 2p spectra were displayed in Fig. 8(e) and (f). A satellite peak (S1) near 860 eV was observed in both two samples, indicating nickel oxides on the cathode surface [33]. However, there is much difference in Ni 2p3/2 signal. The SN-absent sample signal located at 854.2 eV, suggesting a single valence of Ni^{2+}. In contrast with SN-absent sample, a shoulder peak of 856 eV identified the existence of Ni^{3+} in SN-containing sample. In summary, the XPS results prove that the introducing of SN contributes to produce compounds containing Ni^{3+} and Mn^{3+} in the cathode surface. The interaction between electronegativity group CN^- and Ni^{3+}or Mn^{3+} needed for further research. Although it is not accurate to judge the Mn/Ni deposition amount based on the half-peak width area. But the fact can't be ignorable that the area of Mn/Ni peak of 1wt % SN-based electrolyte was respectively 1/3 and 1/2 of commercial electrolyte. It implies

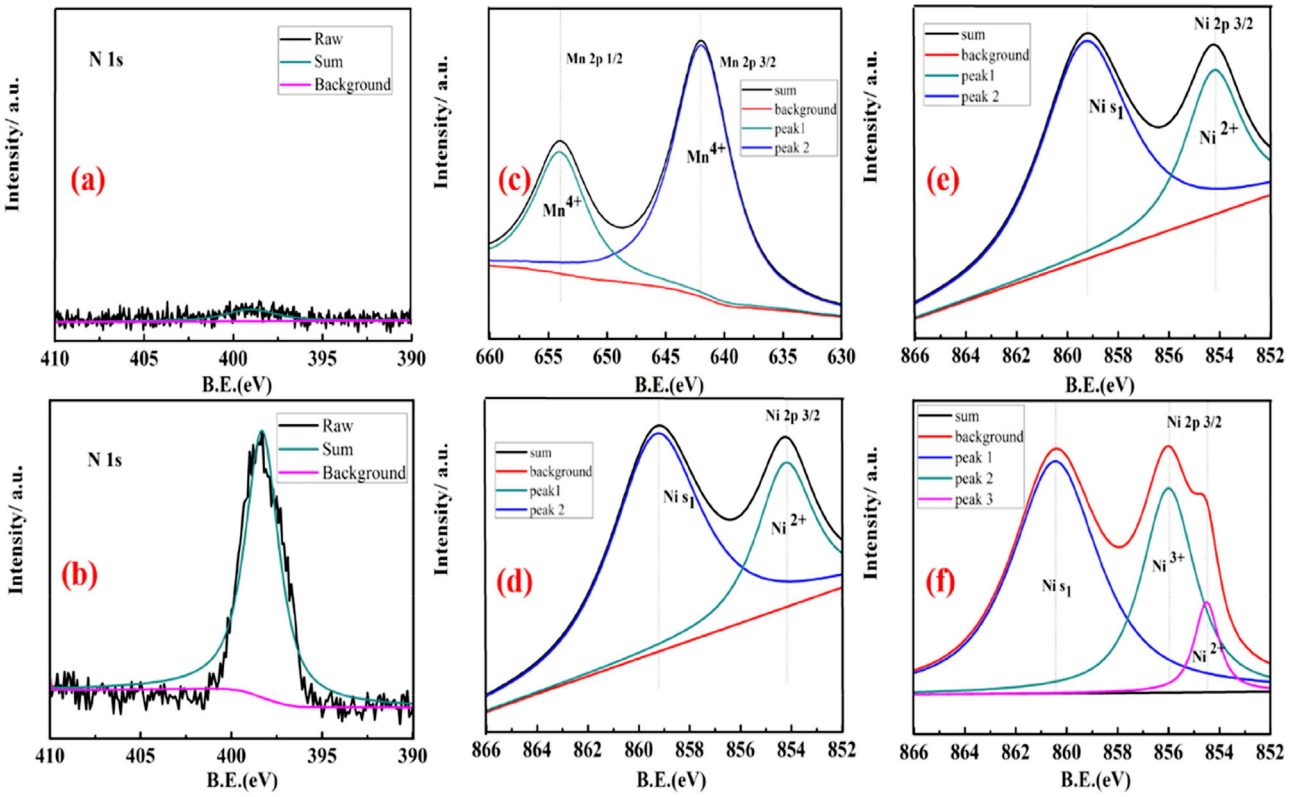

Fig. 8. XPS spectra of the regions of $Li_{1.2}Ni_{0.2}Mn_{0.6}O_2$ after 50 cycles: (a) N1s with commercial electrolyte, (b) N1s with 1wt% SN-based electrolyte, (c) Mn2p with commercial electrolyte, (d) Mn2p with 1wt% SN-based electrolyte, (e) Ni2p with commercial electrolyte, (f) Ni2p with 1wt% SN-based electrolyte.

that SN effectively alleviates Mn/Ni deposition on the cathode to a certain degree.

4. Conclusion

Succinonitrile-based electrolytes improve the cycling performance and thermal stability of the $Li_{1.2}Ni_{0.2}Mn_{0.6}O_2$/Li system in high cut-off voltage in this paper. By performing linear sweep voltammetry (LSV), thermogravimetry (TG) and X-ray photoelectron spectroscopy (XPS), the results showed that the commercial electrolyte containing 1wt % SN has a better thermal stability and wider electrochemical oxidation window to 5.4 V, which is corresponding to the theoretic calculation results. The energies of the LUMO and HOMO of SN are both lower than those of EC and DEC. At a voltage range of 2.0–5.0 V, 1wt % SN-based electrolyte was proved to be the optimal proportion for LNMO batteries. SN also has an outstanding ability to form a CEI layer observed from SEM images, which contributes to the alleviation of Mn/Ni dissolution into electrolyte and deposition on the cathode. Cycling tests of Li/$Li_{1.2}Ni_{0.2}Mn_{0.6}O_2$ half-cells under different upper cut-off voltage confirm that Li/$Li_{1.2}Ni_{0.2}Mn_{0.6}O_2$ half-cells containing 1wt % SN-based electrolyte exhibits a better capacity retention and higher coulombic efficiency than commercial electrolytes. In summary, 1wt % SN-based electrolyte shows a wider electrochemical oxidation stability window and better thermal stability, as well as its good compatibility with LNMO electrodes. As a result, deployment of succinonitrile-based electrolyte can lead to long life and safer lithium-ion batteries for automobile and grid applications.

Acknowledgments

This work is financially supported by the National Science Foundation of China (21373028), Major achievements Transformation Project for Central University in Beijing, National Key Program for Basic Research of China (2015CB251100) and Beijing Science and Technology Project (D151100003015001).

References

[1] M. Hu, X. Pang, Z. Zhou, J. Power Sources 237 (2013) 229–242.
[2] J.M. Lloris, C. Perez Vicente, J.L. Tirado, Electrochem. Solid State Lett. 5 (2002) A234.
[3] F. Zhou, M. Cococcioni, K. Kang, G. Ceder, Electrochem. Commun. 6 (2004) 1144–1148.
[4] L. Yang, B. Ravdel, B.L. Lucht, Electrochem. Solid State Lett. 13 (2010) A95.
[5] L. Hu, Z. Zhang, K. Amine, J. Power Sources 236 (2013) 175–180.
[6] F. Wu, J. Xiang, L. Li, J. Chen, G. Tan, R. Chen, J. Power Sources 202 (2012) 322–331.
[7] F. Wu, Q. Zhu, L. Li, R. Chen, S. Chen, J. Mater. Chem. A 1 (2013) 3659.
[8] J. Xiang, F. Wu, R. Chen, L. Li, H. Yu, J. Power Sources 233 (2013) 115–120.
[9] V. Aravindan, Y.L. Cheah, W.C. Ling, S. Madhavi, J. Electrochem. Soc. 159 (2012) A1435–A1439.
[10] X. Liao, Q. Huang, S. Mai, X. Wang, M. Xu, L. Xing, Y. Liao, W. Li, J. Power Sources 272 (2014) 501–507.
[11] H. Bouayad, Z. Wang, N. Dupré, R. Dedryvère, D. Foix, S. Franger, J.F. Martin, L. Boutafa, S. Patoux, D. Gonbeau, D. Guyomard, J. Phys. Chem. C 118 (2014) 4634–4648.
[12] C.H. Lei, J. Bareño, J.G. Wen, I. Petrov, S.H. Kang, D.P. Abraham, J. Power Sources 178 (2008) 422–433.
[13] L. Zhang, B. Wu, N. Li, D. Mu, C. Zhang, F. Wu, J. Power Sources 240 (2013) 644–652.
[14] L. Chen, Y. Su, S. Chen, N. Li, L. Bao, W. Li, Z. Wang, M. Wang, F. Wu, Adv. Mater. 26 (2014) 6756–6760.
[15] M. Gu, I. Belharouak, J. Zheng, H. Wu, J. Xiao, A. Genc, K. Amine, S. Thevuthasan, D.R. Baer, J.G. Zhang, N.D. Browning, J. Liu, C. Wang, ACS Nano 7 (2013) 760–767.
[16] P. Yan, A. Nie, J. Zheng, Y. Zhou, D. Lu, X. Zhang, R. Xu, I. Belharouak, X. Zu, J. Xiao, K. Amine, J. Liu, F. Gao, R. Shahbazian-Yassar, J.G. Zhang, C.M. Wang, Nano Lett. 15 (2015) 514–522.
[17] C.A. Bunton, J.H. Crabtree, L. Robinson, J. Am. Chem. Soc. 90 (1968) 1258–1265.
[18] Y. Abu-Lebdeh, I. Davidson, J. Power Sources 189 (2009) 576–579.

[19] Y. Abu-Lebdeh, I. Davidson, J. Electrochem. Soc. 156 (2009) A60.
[20] M. Nagahama, N. Hasegawa, S. Okada, J. Electrochem. Soc. 157 (2010) A748.
[21] L.Z. Fan, Y.S. Hu, A.J. Bhattacharyya, J. Maier, Adv. Funct. Mater. 17 (2007) 2800–2807.
[22] K. Meng, K.R. Thampi, ACS Appl. Mater. Interfaces 6 (2014) 20768–20775.
[23] M. Suleman, Y. Kumar, S.A. Hashmi, J. Phys. Chem. B 117 (2013) 7436–7443.
[24] Y.S. Kim, S.H. Lee, M.Y. Son, Y.M. Jung, H.K. Song, H. Lee, ACS Appl. Mater. Interfaces 6 (2014) 2039–2043.
[25] Y.-S. Kim, T.-H. Kim, H. Lee, H.-K. Song, Energy Environ. Sci. 4 (2011) 4038.
[26] G.Y. Kim, R. Petibon, J.R. Dahn, J. Electrochem. Soc. 161 (2014) A506–A512.
[27] A.R. Armstrong, M. Holzapfel, P. Novak, C.S. Johnson, S.H. Kang, M.M. Thackeray, P.G. Bruce, J. Am. Chem. Soc. 128 (2006) 8694–8698.
[28] F. Wu, M. Wang, Y. Su, S. Chen, B. Xu, J. Power Sources 191 (2009) 628–632.
[29] H.-W. Ha, N.J. Yun, K. Kim, Electrochim. Acta 52 (2007) 3236–3241.
[30] J. Jin, H.H. Li, J.P. Wei, X.K. Bian, Z. Zhou, J. Yan, Electrochem. Commun. 11 (2009) 1500–1503.
[31] Y. Qian, Y. Deng, Z. Shi, Y. Zhou, Q. Zhuang, G. Chen, Electrochem. Commun. 27 (2013) 92–95.
[32] S.K. Martha, J. Nanda, G.M. Veith, N.J. Dudney, J. Power Sources 216 (2012) 179–186.
[33] H.W. Nesbitt, D. Legrand, G.M. Bancroft, Phys. Chem. Miner. 27 (2000) 357–366.